Apparent pressure derived from ADEOS-POLDER observations in the oxygen A-band over ocean

Claudine Vanbauce, Jean-Claude Buriez, Frédéric Parol, Bernard Bonnel, G. Sèze, P. Couvert

Apparent pressure derived from ADEOS-POLDER observations in the oxygen A-band over ocean

C. Vanbauce, J.C. Buriez, F. Parol, B. Bonnel

LOA, Université des Sciences et Technologies de Lille, 59655 Villeneuve d'Ascq, France

G. Sèze

LMD, Université de Jussieu, 75252 Paris, France

P. Couvert

LSCE, Centre d'Etudes de Saclay, 91191 Gif-sur-Yvette, France

Abstract. The POLDER radiometer was on board the ADEOS satellite from August 1996 to June 1997. This instrument measures radiances in eight narrow spectral bands of the visible and near infrared spectrum. Two of them are centered on the O_2 A-band in order to infer cloud pressure. By assuming the atmosphere behaves as a pure absorbing medium overlying a perfect reflector, an "apparent" pressure P_{app} is derived from POLDER data. For validation purposes, P_{app} is first compared to the sea-surface pressure P_s for clear-sky conditions; P_{app} is found to be close to P_s (within ~ 30 hPa) for measurements in the sunglint region. For overcast conditions, P_{app} differs from the cloud-top pressure mainly because of multiple scattering inside the cloud. When P_{app} is compared to the cloud pressure determined from brightness temperature measurements, large differences are observed (typically 180 hPa).

Introduction

Yamamoto and Wark [1961] have suggested the use of oxygen A-band absorption to infer cloud pressure. Recently, some theoretical efforts [*Fisher and Grassl*, 1991; *O'Brien and Mitchell*, 1992; *Kuze and Chance*, 1994] and aircraft measurements [*Fisher et al.*, 1991] have been carried out. All these studies have shown that the oxygen A-band is potentially efficient for determining the cloud-top pressure. They have also shown that the main difficulty lies in the photon penetration problem and the influence of ground reflectivity.

The POLDER (POLarization and Directionality of the Earth's Reflectances) [*Deschamps et al.*, 1994] radiometer has two spectral bands centered on the oxygen A-band. It was launched on ADEOS (Advanced Earth Observing Satellite) in August 1996.

This paper presents first results of the apparent pressure derived from ADEOS-POLDER data by using a non-scattering model. This pressure is compared to the meteorological sea-surface pressure for clear-sky conditions and to the cloud pressure deduced from brightness temperature measurements for overcast conditions.

Data

The POLDER instrument on ADEOS is described in *Deschamps et al.* [1994]. It consists of a CCD matrix detector, a rotating filter wheel and a wide field of view lens. When the satellite passes over a target, up to 14 different images are acquired in eight narrow spectral bands of the visible and near infrared spectrum.

The POLDER level 1 products processed by the French Space Center (CNES) consist of calibrated radiances at 6.2 km resolution. The level 2 and 3 products are split in three processing lines: "Earth Radiation Budget (ERB) and clouds", "Ocean color and aerosols over the ocean", "Land surfaces and aerosols over land".

The apparent pressure P_{app} is one of the outputs of the "ERB and clouds" processing line. It is inferred from the differential absorption between the reflectances measured in the narrowband and wideband channels centered at 763 and 765 nm respectively. Practically, P_{app} is calculated as a function of the oxygen transmission derived from these two reflectances after removing ozone and water vapor absorption (see *Buriez et al.* [1997] for further details). The gaseous transmissions are based on line by line simulations using HITRAN'96 spectroscopic data bank [*Rothman et al.*, 1998]. All scattering effects are neglected and the atmosphere is assumed to behave as a pure absorbing medium overlying a perfect reflector located at pressure P_{app}. In addition, the reflectance R^* that would be measured if there was no absorption is derived by assuming it is the same in both channels. These calculations are made for every geographic pixel but the POLDER products correspond to means over super-pixels composed of 9 by 9 pixels (0.5° by 0.5° at the equator).

The interband calibration between the 763 nm and 765 nm channels is expected to be accurate within 1 % [*Hagolle et al.*, 1997]; it corresponds to an absolute accuracy of about 20 hPa on the retrieved pressure. The radiometric noise induces a rms error varying from less than 7 hPa for very bright scenes ($R^* > 50$ %) to more than 60 hPa for very dark scenes ($R^* < 2$ %) ; these values are divided at most by 9 when averaging over a super-pixel. There are however additional uncertainties, mainly due to residual defaults in the stray light correction and in the multi-directional co-registration. The stray light strongly affects the dark scenes while co-registration errors concern scenes with high spatial or angular variability such as heterogeneous clouds and

ocean in the sunglint direction. From these considerations and comparison of values of the super-pixel apparent pressure retrieved for slightly different viewing directions, the overall rms error due to all error sources is estimated to vary from $\leq$ 30 hPa for very bright scenes up to $\sim$ 40 - 60 hPa for very dark scenes.

POLDER data presented here were acquired during the 14 daily overpasses of ADEOS over ocean on November 10, 1996. These data are complemented by brightness temperature measurements from Meteosat and by the sea-surface pressure and meteorological profiles derived from the ECMWF (European Centre for Medium range Weather Forecasts) analysis.
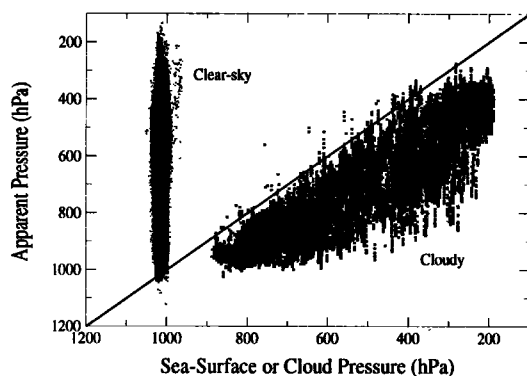
Comparison to sea-surface pressure

First we are interested in the behavior of the apparent pressure derived from POLDER measurements in clear-sky conditions. We select the fully clear-sky super-pixels by using a simple reflectance test. For each pixel and for each viewing direction, the clear-sky reflectance at 865 nm R_{865}^{clear} is estimated from radiative transfer simulations. A super-pixel is declared clear if the measured reflectance R_{865} is weaker than $R_{865}^{clear} + 0.02$ for all the 81 pixels of the super-pixel and for each viewing direction outside the expected region of the solar specular reflection delimited by a cone of half-angle of 30°. A more severe threshold (0 instead of 0.02) reduces the number of selected clear cases but does not change significantly the following results.

For these clear-sky conditions, the POLDER apparent pressure P_{app} is compared to the sea-surface pressure P_s (Figure 1). For the 78,364 selected cases, the mean difference is - 412 hPa with a standard deviation of 144 hPa. Not surprisingly, P_{app} is generally smaller than P_s. Indeed, P_{app} must be equal to P_s only when all of the reflected radiation directly comes from the sea-surface. In the other cases, we would have to take into account the atmospheric effects. In order to illustrate these effects, we consider a simple model where R^* is the sum of the reflectances directly generated by molecular scattering, aerosol scattering and surface reflectance :

$$R^* = R_m + R_a + R_s\, t_{atm}\ ,\qquad (1)$$

where t_{atm} stands for the atmospheric transmittance.

Figure 1. Comparison between the apparent pressure P_{app} derived from POLDER and respectively (i) the meteorological sea-surface pressure P_s for clear-sky pixels and (ii) the cloud pressure P_c derived from Meteosat brightness temperature for cloudy pixels.
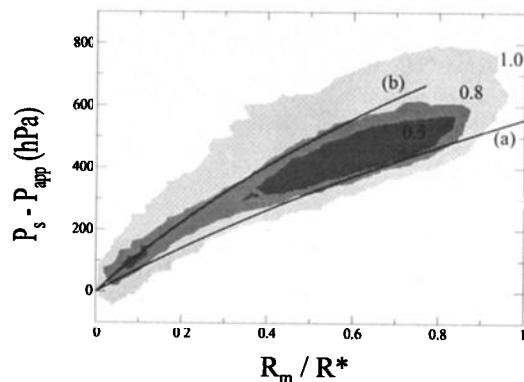
Figure 2. Difference between the apparent pressure and the sea-surface pressure versus the ratio between the calculated molecular reflectance and the measured total reflectance. 100%, 80% and 50% of the cases are situated within the isoline 1.0, 0.8 and 0.5 respectively. The theoretical curves correspond to an air-mass factor $m = 3$. Curve a corresponds to a clean atmosphere. Curve b corresponds to a ratio between the aerosol reflectance and the molecular reflectance equal to 0.3 and a formation pressure equal to 50 hPa.

The reflectance affected by O_2-absorption is formally

$$R^*\, t(P_{app}) = R_m\, t(P_m) + R_a\, t(P_a) + R_s\, t_{atm}\, t(P_s)\qquad (2)$$

where $t(P)$ is the two-path oxygen transmission between the top-of-atmosphere and the pressure P. Writing $\alpha = R_a/R_m$, (1) and (2) give

$$t(P_{app}) = t(P_s)+\{t(P_m) - t(P_s) + \alpha[t(P_a) - t(P_s)]\}\,\frac{R_m}{R^*}.\qquad (3)$$

The molecular reflectance R_m is easily calculable, based on single-scattering approximation ; it is typically ~ 1 %. From line-by-line simulations for standard atmospheres, the pressure P_m is found to hardly decrease (from 470 to 440 hPa) when the air-mass factor increases from 2 to 5. The aerosol reflectance R_a and above all its associated pressure P_a are a lot more uncertain. The aerosol pressure values extend from about 50 hPa for stratospheric aerosol to more than 900 hPa for tropospheric aerosol.

Figure 2 reports the difference P_s - P_{app} versus the ratio between the calculated molecular reflectance R_m and the total reflectance R^* inferred from POLDER measurements. Two theoretical curves are also reported for a typical air-mass factor $m = 3$. Curve a corresponds to a clean atmosphere $(\alpha = 0)$. Curve b corresponds to an aerosol layer with a reflectance ratio $\alpha = 0.3$ and a formation pressure $P_a = 50$ hPa. This curve b can also be obtained for other conditions: for example $P_a = 200$ hPa but $\alpha = 0.38$, or Pa = 900 hPa but $\alpha = 4.3$. However, R_m/R^* is strictly limited by $1/(1+\alpha)$ that is 0.77 for $\alpha = 0.3$ but only 0.19 for $\alpha = 4.3$.

Of course, a fixed value of α whatever the solar and viewing directions is unrealistic. Nevertheless, the comparison between the measurements and these theoretical curves leads to some remarks: the general trend of the observations is rather well represented by the theoretical curves. As expected, the measured difference P_s - P_{app} tends toward 0 when the contribution of the photons reflected by the atmosphere becomes negligible. Deviations from the "mean" curve (not drawn) are

mainly random, with a standard deviation increasing from $\sim$ 30 hPa to 70 hPa when R_m/R^* increases.

On the average, the observations significantly depart from the theoretical clean atmosphere case (curve a). Tropospheric aerosol typically located between 800 and 1000 hPa cannot explain this bias which is observed for large values of R_m/R^*. It could be due to a stratospheric aerosol layer and/or a very tenuous cirrus cloud layer. The stratospheric aerosol contents derived from SAGE (Stratospheric Aerosol and Gas Experiment) measurements are found to be nearly ten times too small to explain such a bias. The frequent occurrence of thin cirrus with reflectance on the order of 1-2 % cannot be excluded but is questionable.

Besides an unlikely failure in the retrieval of the apparent pressure, another explanation could be in part a slight bias in the stray light correction [*Hagolle*, private communication]. Fortunately, such a bias would have a negligible effect in the case of bright clouds as considered in the following.

Comparison to Meteosat data

Now we are interested in the behavior of the apparent pressure in cloudy conditions. A super-pixel is declared overcast if the condition $R_{865} > 0.50$ is satisfied for all the 81 pixels of the super-pixel and for each viewing direction. A large threshold is chosen in order to privilege the clouds that are opaque in the Meteosat infrared channel and to avoid as far as possible the presence of partly cloud-filled pixels.

In this section, are only considered the cloudy pixels observed both from POLDER and from Meteosat within $\pm 1/4$ hour (some trials using GOES instead of Meteosat observations gives similar results). Three ADEOS orbits are concerned on November 10, 1996. For each selected super-pixel, a pressure P_c is derived from the brightness temperature measured in the 11 μm channel of the geostationary satellite by using meteorological profile. Disregarding errors chiefly caused by uncertainties in temperature profile, the pressure P_c is close to the cloud-top pressure when the cloud is opaque. Note however that the auxiliary atmospheric data archived with the POLDER products are given for only eight pressure levels, namely 180, 310, 440, 560, 680, 800, 1000 hPa and the surface level. Therefore the well-known inversion observed near the top of the stratocumulus clouds may be missed in these data ; it can result in a large error in the derivation of the cloud pressure from the observed temperature. In the following, results are thus to be considered cautiously in the case of low-level clouds.

The comparison between the Meteosat cloud pressure P_c and the POLDER apparent pressure P_{app} is reported in Fig. 1. For the 32,471 selected cases, the mean difference is 184 hPa with a standard deviation of 87 hPa. As the reflectance threshold is large enough, no significant variation of the difference as a function of the reflectance is observed. A slight variation of P_{app} with the air-mass factor m is noted. Each super-pixel is observed under several directions to which correspond different values of m; on average, $\partial P_{app}/\partial m \approx$ - 65 hPa.

As expected from theoretical considerations [e.g., *Wu*, 1985], P_{app} is now larger than P_c. Simulations using the Discrete Ordinate Method [*Stammes et al.*, 1988] were performed for various cloudy situations and various solar illumination and viewing conditions. Some exam-
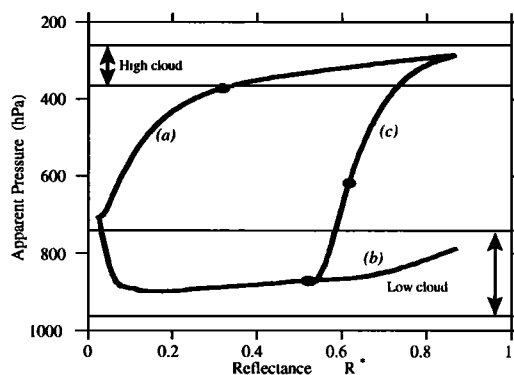
Figure 3. Theoretical curves of the apparent pressure as a function of the reflectance for mono-layered clouds (curves a and b) and for a multi-layered cloud system (curve c) above the ocean. All the clouds are 2 km thick. In cases a and b, the cloud optical thickness varies from 0 to 500. In case c, the high-level cloud optical thickness varies from 0 to 500 while the low-level cloud optical thickness is fixed to 16. The dots correspond to an optical thickness of 16 for both the low and the high cloud. The viewing and the solar angles are $0°$ and $60°$ respectively.

ples are reported in Figure 3. Clouds are assumed to be homogeneous plane-parallel layers. The microphysical model for low-level clouds is a distribution of liquid water drops with an effective radius of 10 μm [*Hansen and Travis*, 1974]. High-level clouds are assumed to be composed of hexagonal ice plates with dimensions L/2R = 15 μm/300 μm [*Brogniez et al.*, 1995]. In Fig. 3, the cloud optical thickness δ varies from 0 to 500. As noted previously, P_{app} differs notably from P_s when $\delta = 0$.

The apparent pressure does not correspond to the cloud top because of multiple scattering inside the cloud. This photon penetration effect remains significant even for cloud optical thickness larger than 100. From many simulations such as those reported in Fig. 3, it appears that for single cloud layers with a typical reflectance value of 50 %, the apparent pressure is generally slightly larger than the mean cloud pressure (i.e. rather toward the cloud bottom than toward the cloud top).

In the case of multi-layered cloud systems, the difference between the apparent and the cloud top pressure is amplified (curve c in Fig.3). Indeed, a large part of the reflected radiation can come from the lower cloud layer. That can explain very large differences between the POLDER apparent pressure and the pressure P_c derived from thermal infrared channels. Note that the brightness temperature technique also can overestimate the cloud-top pressure in case of multiple cloud layers ; if so, the difference between the apparent and the true cloud-top pressure would be still larger than $P_{app} - P_c$.

Note that our simulations agree with the observed variation of the photon penetration with the air-mass factor. Typically, we found $\partial P_{app}/\partial m \approx$ - 30 hPa and - 80 hPa for single and two-layered clouds respectively, to be compared to the observed - 65 hPa.

Conclusion

The first results of the apparent pressure P_{app} derived from ADEOS-POLDER data have been presented. They only concern oceanic situations. Over land, the inter-

pretation of the apparent pressure is even more complicated because the surface reflectivity can present a large spectral variability [Bréon and Bouffiès, 1996].

Under clear-sky conditions, the apparent pressure tends toward the sea-surface pressure (within ~30 hPa) when the contribution of the photons reflected by the atmosphere becomes negligible. Outside the sunglint region, the sea-surface reflectivity is very weak and the apparent pressure is thus highly dependent on the atmosphere composition; the presence of a high-level scattering layer, even very tenuous, can have a significant impact on the measure of the apparent pressure.

Under cloudy conditions, the apparent pressure is greater than the cloud top pressure because of the effect of surface reflectivity and multiple scattering inside the cloud. The measured difference between the POLDER apparent pressure and the cloud top pressure derived from infrared measurements is on the average 180 hPa. Such a difference appears rather large for single cloud layers. However, there is often occurrence of both low and high clouds [Warren et al., 1988]. In this case, very large differences can arise even when the high cloud appears opaque in the thermal infrared window.

Some doubt remains concerning the spectroscopic data and the modeling of the apparent pressure based on line-by-line calculations [Kuze and Chance, 1994; Chance, 1997]. However, forcing the adjustment between the average of the clear-sky observations and the clean-sky simulations (curve a in Fig. 2) would increase the observed differences between the cloud top and the apparent pressure.

The POLDER apparent pressure is thought to be useful for discriminating clear and cloudy pixels and for deriving the cloud pressure. These first results outline that the use of the apparent pressure in the cloud detection has to be made with precautions. For cloudy scenes, even when the sea-surface reflectivity effect is negligible, the apparent pressure is not the cloud top pressure. Its comparison with the actual cloud top pressure (or at least the cloud top derived from thermal infrared measurements) is expected to contain information about the cloud vertical structure. More studies are needed in order to extract this information that could be very useful particularly for the derivation of surface thermal fluxes from satellite observations.

References

Bréon, F. M., and S. Bouffiès, Land surface pressure estimate from measurements in the oxygen A absorption band, J. Appl. Meteor., 35, 69-77, 1996.

Brogniez, G., J.C. Buriez, V. Giraud, F. Parol, and C. Vanbauce, Determination of effective emittance and radiatively equivalent microphysical model of cirrus from ground-based and satellite observations during the International Cirrus Experiment: The 18 October 1989 case study, Mon. Wea. Rev., 123, 1025-1036, 1995.

Buriez, J.C., C. Vanbauce, F. Parol, P. Goloub, M. Herman, B. Bonnel, Y. Fouquart, P. Couvert, and G. Sèze, Cloud detection and derivation of cloud properties from POLDER, Int. J. Remote Sensing, 18, 2785-2813, 1997.

Chance, K.V., Improvement of the O_2 A-band spectroscopic database for satellite-based cloud detection, J. Quant. Spectrosc. Radiat. Transfer, 58 no. 3, 375-378, 1997.

Deschamps, P.Y., F. M. Bréon, M. Leroy, A. Podaire, A. Bricaud, J.C. Buriez, and G. Sèze, The POLDER mission: Instrument characteristics and scientific objectives, IEEE Trans. Geosci. Rem. Sens., 32, 598-615, 1994.

Fisher, J., and H. Grassl, Detection of cloud-top height from backscattered radiances within the O_2 A-band. Part 1: Theoretical study, J. Appl. Meteor., 30, 1245-1259, 1991.

Fisher, J., W. Cordes, A. Schmitz-Peiffer, W. Renger, and P. Mörl, Detection of cloud-top height from backscattered radiances within the O_2 A-band. Part 2: Measurements, J. Appl. Meteor., 30, 1260-1267, 1991.

Hagolle, O., P. Goloub, P.Y. Deschamps, T. Bailleul, J.M. Nicolas, Y. Fouquart, A. Meygret, J.L. Deuzé, M. Herman, F. Parol, and F.-M. Bréon, Results of POLDER in-flight calibration. In Sensors Systems and Next Generation Satellite III, Proc. SPIE 3221, 1997.

Hansen, J.E., and L. D. Travis, Light scattering in planetary atmospheres, Space Sci. Rev., 16, 527-610, 1974.

Kuze, A., and K.V. Chance, Analysis of cloud top height and cloud coverage from satellites using the O_2 A and B bands, J. Geophys. Res., 99, 14481-14492, 1994.

O'Brien, D.M., and R. M. Mitchell, Error estimates for retrieval of cloud-top pressure using absorption in the A band of Oxygen, J. Appl. Meteor., 31, 1179-1192, 1992.

Rothman, L.S., C.P. Rinsland, A. Goldman, S.T. Massie, D.P. Edwards, J.-M. Flaud, A. Perrin, C. Camy-Peyret, V. Dana, J.-Y. Mandin, J. Schroeder, A. McCann, R.R. Gamache, R.B. Wattson, K. Yoshino, K. Chance, K. Jucks, L.R. Brown, V. Nemtchinov, and P. Varanasi, The HITRAN Molecular Spectroscopic Database and HAWKS: 1996 Edition, to be submitted to J. Quant. Spectrosc. Radiat. Transfer, 1998.

Stamnes, K., S.C. Tsay, W. Wiscombe, and K. Jayaweera, Numerically stable algorithm for discrete-ordinate-method radiative transfer in multiple scattering and emitting layered media, Appl. Opt., 27, 2502-2509, 1988.

Warren, S.G., C.J. Hahn, J. London, R.M. Chervin, and R.L. Jenne, Global distribution of total cloud cover and cloud type amounts over the ocean, NCAR Tech. Note TN-317+STR/DOE Tech. Rep. ER-0406, 212 pp., 1988.

Wu, M.C., Remote sensing of cloud-top pressure using reflected solar radiation in the Oxygen A-band, J. Clim.Appl. Meteor., 24, 539-546, 1985.

Yamamoto, G., and D. Q. Wark, Discussion of the letter by R.A. Hanel: "Determination of cloud altitude from a satellite", J. Geophys. Res., 66, 3596, 1961.